Computers and Mathematics with Applications 60 (2010) 1924–1939

Contents lists available at ScienceDirect

Computers and Mathematics with Applications

journal homepage: www.elsevier.com/locate/camwa

Parameter-uniform numerical method for global solution and global normalized flux of singularly perturbed boundary value problems using grid equidistribution

Jugal Mohapatra [a], Srinivasan Natesan [b,*]

[a] Institute of Mathematics and Applications, Bhubaneswar - 751003, India

[b] Department of Mathematics, Indian Institute of Technology Guwahati, Guwahati - 781 039, India

ARTICLE INFO

Article history:
Received 29 December 2009
Received in revised form 20 July 2010
Accepted 20 July 2010

Keywords:
Singularly perturbed convection–diffusion problems
Upwind scheme
Adaptive mesh
Normalized flux
Uniform convergence

ABSTRACT

In this paper, we present the analysis of an upwind scheme for obtaining the global solution and the normalized flux for a convection–diffusion two-point boundary value problem. The solution of the upwind scheme is obtained on a suitable nonuniform mesh which is formed by equidistributing the arc-length monitor function. It is shown that the discrete solution obtained by the upwind scheme and the global solution obtained via interpolation converges uniformly with respect to the perturbation parameter. In addition, we prove the uniform first-order convergence of the weighted derivative of the numerical solution on this nonuniform mesh and the uniform convergence of the global normalized flux on the whole domain. Numerical results are presented that demonstrate the sharpness of our results.

1. Introduction

In this article, we consider the following singularly perturbed boundary value problem (SPBVP):

$$\begin{cases} Lu(x) \equiv -\varepsilon u''(x) - a(x)u'(x) + b(x)u(x) = f(x), \quad x \in \Omega = (0,1), \\ u(0) = s_0, \qquad u(1) = s_1, \end{cases} \tag{1.1}$$

where $0 < \varepsilon \ll 1$ is a small singular perturbation parameter, the functions $a(x)$, $b(x)$, $f(x)$ are sufficiently smooth and s_0, s_1 are given constants. Further, we assume that $2\alpha^* \geq a(x) > 2\alpha > 0$ and $b(x) \geq 0$. Under these assumptions, the above problem (1.1) has a unique solution which exhibits a boundary layer at $x = 0$.

The literature on approximation of the solutions of convection–diffusion problems is large and many finite difference methods have been proposed to approximate the solutions ([1–4], the book [5]) and the global solution with the normalized flux [6,7]. But at the same time there are less number of research articles for approximating the derivatives [8–10]. Such approximations are desirable in certain applications, for example, normal derivatives are required to compute the skin friction coefficients and to calculate the stress intensity factors. There are only a few articles that consider finite difference approximations of derivatives of solutions of convection–diffusion problems including [8,9] and the recent book [11]. In [8] the approximation of the unweighted derivative is discussed only outside the layer while in [9], the authors used special kinds of nonuniform meshes namely piecewise-uniform Shishkin mesh and Bakhvalov mesh to derive the derivative approximation on the entire domain while the model equation is in conservative form. The limitation of these kinds of meshes is that they require a considerable amount of information about the exact solution before solving the problem which is not always available.

* Corresponding author. Tel.: +91 3612582613; fax: +91 3612582649.
E-mail addresses: jugal@iitg.ernet.in (J. Mohapatra), natesan@iitg.ernet.in (S. Natesan).

0898-1221/$ – see front matter © 2010 Elsevier Ltd. All rights reserved.
doi:10.1016/j.camwa.2010.07.026

In this paper, we consider the model equation as given in (1.1) and obtain a similar result on a suitable nonuniform mesh known as *adaptive grids*. This approach has the advantage that it can be applied using little or no *a priori* information about the solution. For singular perturbation problems the aim is to cluster automatically the grid points within the boundary layer and an obvious choice of adaptivity criterion is therefore the solution gradient [1,12,4]. There are certain results for adaptive mesh approach to the solution of singular perturbation problems where the upwind finite difference scheme is applied on a nonuniform mesh formed by equidistributing the arc-length monitor function $M(x) = \sqrt{1 + |u'(x)|^2}$ [1,13,4].

The rest of the paper is organized as follows: Section 2 recalls pertinent properties of the solution $u(x)$ of (1.1). In Section 3, we describe the upwind scheme, the generation of the adaptive grids and some technical results that are used later. We prove the estimates for the local truncation error, the bounds for the weighted derivative errors and the convergence analysis of the numerical solution obtained by the upwind scheme on the adaptive grid in Section 4. The convergence of the global solution via interpolation and the error in the global normalized flux are also discussed in the same section. Finally, Section 5 gives some numerical examples that confirm the theoretical error estimates.

1.1. Notations

For any mesh function ϕ_i, we define the following norms

$$\|\phi\| = \max_{i=0,\ldots,N} |\phi_i| \quad \text{and} \quad \|\phi\|_* = \max_{i=1,\ldots,N-1} \left| \sum_{j=i}^{N-1} h_{j+1}\phi_i \right|.$$

Note that

$$\|\phi\|_* \le \|\phi\| \quad \text{and} \quad \|D^-\phi\|_* \le 2\|\phi\|,$$

where D^- is the backward difference operator as defined in (3.1). Throughout this paper C denotes a generic positive constant independent of the grid points x_j and the parameters ε and N (the number of mesh intervals) which can take different values at different places, even in the same argument. A subscripted C (*i.e.*, C_1) is a constant that is independent of ε and of the nodal points x_j, but whose value is fixed. Whenever we write $\phi = \mathcal{O}(\psi)$, we mean that $|\phi| \le C|\psi|$. To simplify the notation, we set $g_j = g(x_j)$ for any function g, while g_j^N denotes an approximation of g at x_j.

Throughout this paper, we assume that

$$\varepsilon \le CN^{-1} \tag{1.2}$$

as is generally the case of discretization of convection–diffusion problems. It is worthwhile to mention that this assumption is not a restriction in practical situations. This inequality is used in the proof of some theorems.

2. Continuous problem

Lemma 2.1 (*Maximum Principle*). *Let v be a smooth function satisfying $v(0) \ge 0, v(1) \ge 0$ and $Lv(x) \ge 0, \ \forall x \in \Omega$, then $v(x) \ge 0, \ \forall x \in \overline{\Omega}$.*

Proof. Let $x^* \in \overline{\Omega}$ be such that $v(x^*) = \min v(x), x \in \overline{\Omega}$ and assume that $v(x^*) < 0$. Clearly $x^* \notin \{0, 1\}$ and $v'(x^*) = 0$ and $v''(x^*) \ge 0$. Now consider

$$Lv(x^*) \equiv -\varepsilon v''(x^*) - a(x^*)v'(x^*) + b(x^*)v(x^*) < 0$$

which is a contradiction to our assumption. Hence $v(x) \ge 0, \forall x \in \overline{\Omega}$. □

An immediate consequence of the maximum principle is the following stability estimate.

Lemma 2.2. *If u is the solution of the boundary value problem (1.1), then*

$$\|u\| \le \alpha^{-1}\|f\| + \max\{|s_0|, |s_1|\}. \tag{2.1}$$

Proof. Consider the following barrier function

$$\psi^{\pm}(x) = \left[\left(\frac{1-x}{\alpha}\right)\|f\| + \max\{|s_0|, |s_1|\}\right] \pm u(x).$$

It is easy to check that $\psi^{\pm}(x) \ge 0$ at $x = 0, 1$. Now from (1.1)

$$\begin{aligned} L\psi^{\pm}(x) &= -\varepsilon\left(\psi^{\pm}(x)\right)'' - a(x)\left(\psi^{\pm}(x)\right)' + b(x)\psi^{\pm}(x) \\ &= \frac{a(x)}{\alpha}\|f\| + b(x)\left[\left(\frac{1-x}{\alpha}\right)\|f\| + \max\{|s_0|, |s_1|\}\right] \pm Lu(x) \\ &\ge \left[\|f\| \pm f(x)\right] + b(x)\left[\left(\frac{1-x}{\alpha}\right)\|f\| + \max\{|s_0|, |s_1|\}\right] \\ &\ge 0. \end{aligned}$$

Thus by applying the maximum principle (Lemma 2.1), we can conclude that $\psi^{\pm}(x) \geq 0, \forall x \in \overline{\Omega}$, which is the required result. □

Lemma 2.3. *The solution $u(x)$ and its derivatives of the BVP (1.1) satisfy the following bounds:*

$$|u^{(k)}(x)| \leq C\left(1+\varepsilon^{-k}\exp(-\alpha x/\varepsilon)\right), \quad k=0,1,2,3,\ x\in\overline{\Omega}. \tag{2.2}$$

Proof. One can prove this lemma by following the method of proof as given in [14]. □

Let us decompose the solution of (1.1) into regular and singular parts as follows:

$$u(x,\varepsilon) = v(x,\varepsilon) + w(x,\varepsilon). \tag{2.3}$$

Now $v(x,\varepsilon)$ can be written in an asymptotic expansion as

$$v(x,\varepsilon) = v_0(x) + \varepsilon v_1(x) + \varepsilon^2 v_2(x),$$

where v_0, v_1 and v_2 are respectively the solutions of the following problems:

$$\begin{cases} a(x)v_0'(x) + b(x)v_0(x) = -f(x), & v_0(1) = s_1, \\ a(x)v_1'(x) + b(x)v_1(x) = -v_0''(x), & v_1(1) = 0, \\ Lv_2(x) = v_1''(x), & v_2(0) = 0, \quad v_2(1) = 0. \end{cases} \tag{2.4}$$

Hence, the regular component of the solution satisfies the BVP:

$$Lv(x) = f(x), \qquad v(0) = v_0 + \varepsilon v_1(0), \qquad v(1) = s_1, \tag{2.5}$$

and the singular component satisfies:

$$Lw(x) = 0, \qquad |w(0)| \leq C, \qquad w(1) = 0, \tag{2.6}$$

where $w(0)$ depends on v and its derivatives which are bounded uniformly in ε.

Lemma 2.4. *For sufficiently small ε and $0 \leq k \leq 3$, the derivatives of v and w satisfy the following bounds:*

$$\begin{aligned} &|v^{(k)}(x)| \leq C\left(1+\varepsilon^{3-k}\right), \\ &|w^{(k)}(x)| \leq C\varepsilon^{-k}\exp\left(-\alpha x/\varepsilon\right), \quad \forall x\in\overline{\Omega}. \end{aligned} \tag{2.7}$$

Proof. The proof can be found in [11]. □

3. Numerical scheme and nonuniform grids

3.1. Discrete problem

Consider the difference approximation of (1.1) on a nonuniform grid $\overline{\Omega}^N = \{x_j\}_{j=0}^N$ and denote $h_j = x_j - x_{j-1}$. For a mesh function Z_j, we define the following difference operators:

$$D^+Z_j = \frac{Z_{j+1}-Z_j}{h_{j+1}}, \qquad D^-Z_j = \frac{Z_j - Z_{j-1}}{h_j}, \qquad D^+D^-Z_j = \frac{2}{h_j+h_{j+1}}\left(D^+Z_j - D^-Z_j\right). \tag{3.1}$$

The upwind finite difference scheme for (1.1) takes the form

$$\begin{cases} L^N U_j^N \equiv -\varepsilon D^+D^-U_j^N - a_j D^+U_j^N + b_j U_j^N = f_j, \quad 1 \leq j \leq N-1, \\ U_0^N = s_0, \qquad U_N^N = s_1. \end{cases} \tag{3.2}$$

Eq. (3.2) can be expressed in the following form of system of algebraic equations

$$\begin{cases} -r_j^- U_{j-1}^N + r_j^c U_j^N - r_j^+ U_{j+1}^N = f_j, \quad j = 1,\ldots,N-1, \\ U_0^N = s_0, \qquad U_N^N = s_1, \end{cases} \tag{3.3}$$

where

$$r_j^- = \frac{2\varepsilon}{h_j(h_j+h_{j+1})}, \qquad r_j^c = \frac{2\varepsilon}{h_j h_{j+1}} + \frac{a_j}{h_{j+1}} + b_j, \qquad r_j^+ = \frac{2\varepsilon}{h_{j+1}(h_j+h_{j+1})} + \frac{a_j}{h_{j+1}}.$$

In the tri-diagonal system (3.3), the off-diagonal entries have the following properties:

$$r_j^- > 0, \qquad r_j^+ > 0, \quad j = 1,\ldots,N-1,$$

and

$$r_j^c + r_j^- + r_j^+ \geq 0, \quad \text{for } j = 1, \ldots, N-1, \tag{3.4}$$

which imply that the stiffness matrix is an M-matrix.

Now we have to find the bound of the truncation error. Set

$$A\phi(x) = \varepsilon\phi'(x) + a(x)\phi(x). \tag{3.5}$$

In the discrete form, the above upwind scheme (3.2) can be written as

$$L^N U_j^N \equiv \left(-D^+(A^N) + b_j\right)U_j^N = f_j, \tag{3.6}$$

where the discrete operator A^N (corresponding to the continuous operator A) is defined by

$$A^N\phi_j = \varepsilon D^-\phi_j + a_j\phi_j. \tag{3.7}$$

Now from (1.1) and (3.5), we obtain

$$\frac{1}{h_{j+1}}\int_{x_j}^{x_{j+1}} f(x)\mathrm{d}x = -D^+(A^N U_j^N) + b_j U_j^N. \tag{3.8}$$

So from (3.6) and (3.8), we have

$$\left| f_j - \frac{1}{h_{j+1}}\int_{x_j}^{x_{j+1}} f(x)\mathrm{d}x \right| \leq CN^{-1}. \tag{3.9}$$

The truncation error is defined by

$$\tau_j \equiv L^N(U_j^N - u(x_j)) = D^+\left[A^N U_j^N - Au(x_j)\right] + \left[f_j - \frac{1}{h_{j+1}}\int_{x_j}^{x_{j+1}} f(x)\mathrm{d}x\right]. \tag{3.10}$$

Using the decomposition (2.3), we have

$$A^N U_j^N - Au(x_j) = \varepsilon[D^- U_j^N - u'(x_j)] = \varepsilon[D^- V_j^N - v'(x_j)] + \varepsilon[D^- W_j^N - w'(x_j)] =: \varepsilon\mu_j + \eta_j, \tag{3.11}$$

where V_j^N and W_j^N are the discrete approximations of $v(x_j)$ and $w(x_j)$ respectively. Applying the mean-value theorem and using (2.7), we get the following:

$$|\mu_j| = |D^- V_j^N - v'(x_j)| \leq Ch_j \leq CN^{-1}, \tag{3.12}$$

and

$$|\eta_j| = \varepsilon|D^- W_j^N - w'(x_j)| \leq C\left\{\min\left\{\frac{h_j}{\varepsilon}, 1\right\}\exp\left(\frac{-\alpha x_{j-1}}{\varepsilon}\right)\right\}. \tag{3.13}$$

Lemma 3.1. *For the truncation error τ_j defined by $\tau_j = \varepsilon D^+\mu_j + D^+\eta_j + \mathcal{O}(N^{-1})$, the following inequality holds:*

$$\|\tau_j\|_* \leq C\max_{1\leq j\leq N}\left\{\min\left\{\frac{h_j}{\varepsilon}, 1\right\}\exp\left(\frac{-\alpha x_{j-1}}{\varepsilon}\right)\right\} + CN^{-1}. \tag{3.14}$$

Proof. Using the bounds of η_j and μ_j given by (3.12) and (3.13) in (3.11) and combining with (3.9), we can obtain the required estimate. □

3.2. Grid equidistribution

A commonly used technique in adaptive grid generation is based on the idea of equidistribution. A grid Ω^N is said to be equidistributing, if

$$\int_{x_{j-1}}^{x_j} M\big(u(s), s\big)\mathrm{d}s = \int_{x_j}^{x_{j+1}} M\big(u(s), s\big)\mathrm{d}s, \quad j = 1, \ldots, N-1, \tag{3.15}$$

where $M(u(x), x) > 0$ is called the monitor function. Equivalently, (3.15) can be expressed as

$$\int_{x_{j-1}}^{x_j} M\big(u(s), s\big)\mathrm{d}s = \frac{1}{N}\int_0^1 M\big(u(s), s\big)\mathrm{d}s, \quad j = 1, \ldots, N-1. \tag{3.16}$$

For practical purposes, it is common to use monitor functions which are bounded away from zero to maintain a sensible distribution of mesh points throughout the domain. Here, we consider the scaled arc-length monitor function

$$M\big(u(x), x\big) = \sqrt{1 + (u'(x))^2}, \tag{3.17}$$

which is bounded below by unity. The optimal choice of the monitor function depends on the problem being solved, the numerical discretization being used, and the norm of the error that is to be minimized. In practice, the monitor function is often based on a simple function of the derivatives of the unknown solution. For more details about the equidistribution principle and the choice of monitoring functions, one can refer the articles [1,12].

Remark 3.2. One desirable property of the monitor function is that there exist some positive constants $C_1 \le C_2$ such that

$$C_1 \le M(u(x), x) \quad \text{and} \quad \int_0^1 M(u(x), x)\mathrm{d}x \le C_2.$$

Now combining the above with (3.16), we have $h_j \le (C_2/C_1)N^{-1}$, $j = 1, \ldots, N-1$.

To simplify the treatment, we construct the monitor function (3.17) in terms of the exact solution of (1.1). Now equidistribution can also be thought of as giving rise to a mapping $x = x(\xi)$ relating a computational coordinate $\xi \in [0, 1]$ to the physical coordinate $x \in [0, 1]$ defined by

$$\int_0^{x(\xi)} M\big(u(s), s\big)\mathrm{d}s = \xi \int_0^1 M\big(u(s), s\big)\mathrm{d}s = \xi\ell, \tag{3.18}$$

where ℓ is the length of u over $\overline{\Omega}$. Now

$$\frac{\mathrm{d}x}{\mathrm{d}\xi} = \frac{\ell}{\sqrt{1 + (u'(x))^2}}.$$

More precisely, we have

$$x_j = \int_0^{\xi_j} \frac{\ell}{\sqrt{1 + u'(s)^2}}\mathrm{d}s, \quad \xi_j = \frac{j}{N},\ j = 0, \ldots, N. \tag{3.19}$$

Hence, the step sizes of the mesh are given by

$$h_j = x_j - x_{j-1} = \int_{\xi_{j-1}}^{\xi_j} \frac{\ell}{\sqrt{1 + (u'(s))^2}}\mathrm{d}s. \tag{3.20}$$

For truly adaptive algorithm, the monitor function has to be approximated from the numerical solution. Let U_j^N be the piecewise linear interpolant of knots $(x_j, u(x_j))$. From equidistribution principle (3.15), we have

$$\big[1 + (D^- U_j^N)^2\big]\mathrm{d}x^2 = (\ell\mathrm{d}\xi)^2.$$

In other words, we can construct the mesh from (3.16) as the solution of the following nonlinear system of equations:

$$\begin{cases} (x_{j+1} - x_j)^2 + (U_{j+1}^N - U_j^N)^2 = (x_j - x_{j-1})^2 + (U_j^N - U_{j-1}^N)^2, \quad j = 1, \ldots, N-1, \\ x_0 = 0, \qquad x_N = 1. \end{cases} \tag{3.21}$$

The system of Eqs. (3.2) and (3.21) are solved simultaneously to obtain the solution U_j^N and the grids x_j. Note that although (3.2) represents a linear set of equations for U_j^N, the fact that for the grid we require to equidistribute a monitor function based on U_j^N in (3.16) is nonlinearly linked to the solution.

Lemma 3.3. *If the mesh $\overline{\Omega}^N$ is generated by (3.21), then*

- *There are $\mathcal{O}(N)$ grid points inside the boundary layer $(0, x_K)$. Moreover, $h_j \le C\varepsilon$ for $j \le K$.*
- *There are $\mathcal{O}(1)$ grid points inside the transition region (x_K, x_J) where $\mathcal{O}(1)$ is independent of ε and N.*
- *There are $\mathcal{O}(N)$ grid points inside the regular region $(x_J, 1)$ and $h_j \le CN^{-1}$ for $j \ge J+1$, where $|u'(x)| \gg 1$ if $x < x_J$ and $|u'(x)| = \mathcal{O}(1)$ if $x > x_J$.*

Proof. The proof can be found in [4]. □

4. Convergence analysis

4.1. Local truncation error

Lemma 4.1. *The truncation error defined in (3.10) has the following bound:*

$$|\tau_j| \leq \frac{C}{\varepsilon N} \exp\left(\frac{-\alpha x_j}{\varepsilon}\right). \tag{4.1}$$

Proof. For any function $\psi \in \mathcal{C}^3(\overline{\Omega})$, we have the following bounds (See [14]):

$$\left|\left(D^+ - \frac{\mathrm{d}}{\mathrm{d}x}\right)\psi(x_j)\right| \leq \frac{1}{x_{j+1}-x_j}\int_{x_j}^{x_{j+1}} (x_{j+1}-s)\psi''(s)\mathrm{d}s,$$

$$\left|\left(D^+D^- - \frac{\mathrm{d}^2}{\mathrm{d}x^2}\right)\psi(x_j)\right| \leq \frac{1}{x_{j+1}-x_{j-1}}\left[\frac{1}{h_{j+1}}\int_{x_j}^{x_{j+1}} (x_{j+1}-s)^2\psi'''(s)\mathrm{d}s - \frac{1}{h_j}\int_{x_{j-1}}^{x_j} (s-x_{j-1})^2\psi'''(s)\mathrm{d}s\right]. \tag{4.2}$$

Using the Taylor series expansion and (4.2), the truncation error (3.10) can be expressed as

$$\begin{aligned}\tau_j = {} & \frac{-\varepsilon}{h_j+h_{j+1}}\left[\frac{1}{h_{j+1}}\int_{x_j}^{x_{j+1}} (x_{j+1}-s)^2u'''(s)\mathrm{d}s - \frac{1}{h_j}\int_{x_{j-1}}^{x_j} (s-x_{j-1})^2u'''(s)\mathrm{d}s\right] \\ & + \frac{a_j}{h_{j+1}}\int_{x_j}^{x_{j+1}} (x_{j+1}-s)u''(s)\mathrm{d}s,\end{aligned} \tag{4.3}$$

from which we obtain the following bound

$$|\tau_j| < \varepsilon\int_{x_{j-1}}^{x_{j+1}} |u'''(s)|\mathrm{d}s + C\int_{x_{j-1}}^{x_{j+1}} |u''(s)|\mathrm{d}s. \tag{4.4}$$

If we invoke the derivative bounds of the continuous solution (2.2) in the first term, the above expression becomes

$$|\tau_j| < C\int_{x_{j-1}}^{x_{j+1}} |u''(s)|\mathrm{d}s. \tag{4.5}$$

From (3.19), we have

$$\begin{aligned}|\tau_j| &\leq C\ell\int_{\xi_{j-1}}^{\xi_{j+1}} \frac{|u''(x)|}{\sqrt{1+u'(x)^2}}\mathrm{d}\xi \\ &\leq \frac{C}{\varepsilon}\int_{\xi_{j-1}}^{\xi_{j+1}} \frac{|u'(x)|}{\sqrt{1+u'(x)^2}}\mathrm{d}\xi.\end{aligned} \tag{4.6}$$

From Lemma 2.3, we know that $|u'(x)| = \mathcal{O}(1/\varepsilon)$. Using this bound of the solution, we can get constants C_3 and C_4 such that

$$\frac{C_3}{\varepsilon}\exp\left(\frac{-\alpha^* x}{\varepsilon}\right) \leq u'(x) \leq \frac{C_4}{\varepsilon}\exp\left(\frac{-\alpha x}{\varepsilon}\right),$$

holds. Now (4.6) can be written as

$$\begin{aligned}|\tau_j| &\leq \frac{C}{\varepsilon}\int_{\xi_{j-1}}^{\xi_{j+1}} \frac{\frac{C_4}{\varepsilon}\exp\left(\frac{-\alpha x}{\varepsilon}\right)}{\sqrt{1+\left(\frac{C_3}{\varepsilon}\right)^2\exp\left(\frac{-2\alpha^* x}{\varepsilon}\right)}}\mathrm{d}\xi \\ &\leq \frac{C}{\varepsilon N}\frac{\frac{C_4}{\varepsilon}\exp\left(\frac{-\alpha x_j}{\varepsilon}\right)}{\sqrt{1+\left(\frac{C_3}{\varepsilon}\right)^2\exp\left(\frac{-2\alpha^* x_j}{\varepsilon}\right)}} \\ &\leq R_j\exp\left(\frac{-\omega x_j}{\varepsilon}\right)\end{aligned} \tag{4.7}$$

where $0 < \omega < 1$ is independent of ε, N and $R_j = \frac{C}{\varepsilon N}\frac{(C_4/\varepsilon)\exp\left(-(\alpha-\omega)x_j/\varepsilon\right)}{\sqrt{1+(C_3/\varepsilon)^2\exp\left(-2\alpha^* x_j/\varepsilon\right)}}$.

Let us denote $y_j = (C/\varepsilon)\exp(-\alpha x_j/\varepsilon)$, $g(y) = y/\sqrt{1+y^2}$ which is an increasing function in $[0, y^*]$ where $y^* = \sqrt{(1-\omega)/\omega}$. Since $\omega = \mathcal{O}(1)$, we have $y^* = \mathcal{O}(\omega)$ and hence $g(y^*) = \mathcal{O}(1)$. Therefore, we can express

$$R_j \le \frac{C}{\varepsilon N} g(y_j) \le \frac{C}{\varepsilon N} g(y^*) \le \frac{C}{\varepsilon N},$$

and hence,

$$|\tau_j| \le \frac{C}{\varepsilon N} \exp\left(\frac{-\alpha x_j}{\varepsilon}\right),$$

which is the required result. □

Let us define the piecewise (0, 1)-Padé approximation of $\exp(-\alpha x_j/\varepsilon)$ by

$$S_0 = 1, \qquad S_j = \prod_{k=1}^{j} \left(1 + \frac{\alpha h_k}{\varepsilon}\right)^{-1}, \quad j = 1, \ldots, N, \tag{4.8}$$

then

$$S_j \ge \exp\left(\frac{-\alpha x_j}{\varepsilon}\right).$$

Define the parameter $\sigma = \varepsilon \ln N$, then $\exp(-\sigma/\varepsilon) = N^{-1}$. In other words, we can say that

$$\left(1 + \frac{H}{\varepsilon}\right)^{-1} \approx \exp\left(\frac{-H}{\varepsilon}\right), \quad \text{if } \frac{H}{\varepsilon} \ll 1.$$

4.2. Convergence of the numerical solution

Before deriving the error estimate for the numerical solution, we provide some lemmas which are the prerequisites for the main result.

Lemma 4.2 (*Discrete Comparison Principle*). *If $L^N V_j < L^N Z_j$ for $1 \le j \le N-1$ with $V_0 < Z_0$ and $V_N < Z_N$, then $V_j < Z_j$ for $0 \le j \le N$.*

Proof. From (3.4), it is clear that the matrix associated with the discrete operator L^N is an M-matrix and therefore has a positive inverse. Hence, the result follows. □

Lemma 4.3. *The mesh functions S_j satisfy the following property: for $j = 1, \ldots, N-1$, there exist a constant C, such that*

$$L^N S_j \ge \frac{C}{\max\{\varepsilon, h_{j+1}\}} S_j. \tag{4.9}$$

Proof. One can find the proof in [12]. □

The following lemma provides the two-sided bound for S_j.

Lemma 4.4. *The grid functions S_j defined in (4.8) satisfy*

$$\exp\left(\frac{-\alpha x_j}{\varepsilon}\right) < S_j < C \exp\left(\frac{-\alpha x_j}{\varepsilon}\right), \quad j = 1, \ldots, N-1. \tag{4.10}$$

Proof. One can see the detailed proof in [12,3]. □

The following theorem shows the ε-uniform convergence of the upwind scheme.

Theorem 4.5. *Let $u(x)$ and U_j^N be respectively the exact solution of (1.1) and the discrete solution of (3.2) on the grids defined by (3.21). Then, the following estimate holds:*

$$\max_{0 \le j \le N} |u(x_j) - U_j^N| \le CN^{-1}. \tag{4.11}$$

Proof. The proof is given in [3]. □

4.3. Error in the normalized flux

In this section, we shall derive the bounds on the ε-weighted derivative errors $\{\varepsilon E_j\}$ defined by $E_j = D^- e_j = (e_j - e_{j-1})/h_j$, where e_j denotes the pointwise errors.

Before we derive the bound of the weighted derivatives, let us prove the following lemmas.

Lemma 4.6. *Let the mesh functions z_j and ϕ_j satisfy $L^N z_j = \phi_j$ for $j = 1, \ldots, N-1$ with $z_0 = z_N = 0$, then*

$$\|z\| \leq \frac{2\|\phi\|_*}{\alpha} \quad \text{and} \quad \varepsilon\|D^- z\| \leq \left(2 + \frac{2\alpha}{\alpha^*}\right)\|\phi\|_*.$$

Proof. One can refer [9] for the proof. □

Lemma 4.7. *For $j = 1, \ldots, N$, there exist positive constants C_5 and C_6 such that if*

$$S_j \geq C_5\varepsilon, \tag{4.12}$$

for some j, then

$$M_j = M(U_j^N, x_j) \geq |D^- U_j^N| \geq \frac{C_6 S_j}{\varepsilon}. \tag{4.13}$$

Proof. We have $u = v + w$, where $|v'(x)| \leq C$ and $|w'(x)| \leq w(0)\varepsilon^{-1}\exp(-x/\varepsilon)$. If $S_j \geq C_5\varepsilon$, then we have $S_j/(C_5\varepsilon) \geq 1$. We know that the total arc-length ℓ is of $O(1)$ and it does not change significantly. Now

$$1 \leq \ell = \sum_{j=1}^{N} \sqrt{|U_j - U_{j-1}|^2 + |x_j - x_{j-1}|^2} \leq C_2, \tag{4.14}$$

where $C_2 = 1 + 2\|f\|$. If $\exp(-x/\varepsilon) \geq C_5\varepsilon$ for some x, then using the bounds of $|v'(x)|$ and $|w'(x)|$, we can claim that

$$|u'(x)| \geq C\varepsilon^{-1}\exp(-x/\varepsilon).$$

Now combining $M_j \geq |D^- U_j^N|$ with the above inequality, we can find a constant C_6 such that (4.13) holds. □

Let $\lambda_j = C_2/(C_6 S_j N)$. Using the assumptions (1.2) and (4.12), it is easy to check that $|\lambda_j| \leq C$.

Lemma 4.8. *Let $\varepsilon \leq CN^{-1}$, then*

(i) *For any $[t_1, t_2] \subseteq [0, x_j]$ such that $\ell[t_1, t_2] = \ell/N$, where $\ell[t_1, t_2]$ represents the arc-length of the solution curve in $[t_1, t_2]$, then we have $|t_2 - t_1| \leq \varepsilon\lambda_j$.*
(ii) *If $x_i \geq \varepsilon\lambda_j$, then $\ell[0, x_j] \geq \ell/N$.*

Proof. We know from the definition that

$$\begin{aligned}\ell[t_1, t_2] &= \int_{t_1}^{t_2} \sqrt{1 + u'(s)^2}\,ds \\ &\geq |t_2 - t_1| \min_{1\leq j\leq N} |D^- U_j^N|.\end{aligned}$$

Again for $j \leq i$, $S_j \geq S_i$ and $S_i \geq C_5\varepsilon$, so $S_j \geq C_5\varepsilon$. Now using Lemma 4.7, we have

$$\ell[t_1, t_2] \geq |t_2 - t_1|\frac{C_6 S_j}{\varepsilon}. \tag{4.15}$$

Given that $[t_1, t_2] \subseteq [0, x_j]$ and $\ell[t_1, t_2] = \ell/N$. Hence using (4.14) and (4.15), we can write

$$|t_2 - t_1| \leq \frac{\varepsilon\ell[t_1, t_2]}{C_6 S_j} = \frac{\varepsilon\ell}{C_6 S_j N} \leq \varepsilon\lambda_j.$$

(ii) Set $[t_1, t_2] = [0, x_j]$. From (4.15), we have

$$\ell[0, x_j] \geq \frac{x_j C_6 S_j}{\varepsilon} \geq C_6\lambda_j S_j = \frac{C_5}{N} \geq \frac{\ell}{N},$$

and hence, the lemma is proved. □

Lemma 4.9. *There exist a constant C independent of ε such that*

$$\min\left\{\frac{h_j}{\varepsilon}, 1\right\}\exp\left(\frac{-\alpha x_{j-1}}{\varepsilon}\right) \leq CN^{-1},$$

holds.

Proof. Let J be the largest value of j such that $x_{J-1} \leq \sigma - C_7\varepsilon$. In other words, we have

$$x_{j-1} \leq \sigma - C_7\varepsilon < x_J < \sigma - (C_7 - C_8)\varepsilon, \tag{4.16}$$

where C_7, C_8 satisfy

$$C_7 > C_8 \geq \frac{C_2}{C_5C_6} \quad \text{and} \quad \exp(C_7 - C_8) > C_5(1 + C_2). \tag{4.17}$$

We know that

$$S_J \geq \exp\left(\frac{-x_J}{\varepsilon}\right) \geq \exp\left(\frac{-[\sigma - (C_7 - C_8)\varepsilon]}{\varepsilon}\right) \geq \frac{\exp(C_7 - C_8)}{N}.$$

Combining (4.17) with the assumption $\varepsilon < N^{-1}$, we have $S_J \geq C_2/N \geq C_5\varepsilon$. So

$$x_J > \sigma - C_7\varepsilon = \varepsilon(\ln N - C_7) \geq C_8\varepsilon. \tag{4.18}$$

For sufficiently large N, from (4.16) and (4.17), we have

$$\varepsilon\lambda_J = \frac{C_2\varepsilon}{C_6S_JN} \leq \frac{C_2\varepsilon}{C_2C_6} \leq C_8\varepsilon. \tag{4.19}$$

We know that $|\lambda_J| \leq C_7$, so we can write

$$x_{j-1} \leq \sigma - (C_7 + C_8)\varepsilon = (\sigma - C_7\varepsilon) - C_8\varepsilon. \tag{4.20}$$

From (4.16) and (4.18), we have $x_{j-1} \leq x_J - \varepsilon\lambda_J$. As $x_{j-1} < x_J$, we can have

$$h_{j-1} = x_j - x_{j-1} = x_J - x_{j-1} \leq \varepsilon\lambda_J \leq C_7\varepsilon. \tag{4.21}$$

From (4.20) and (4.21), we get $x_j \leq \sigma - C_7\varepsilon$. Since $j < J$, then $S_j \geq S_J$ and combining with (4.21), we obtain $h_j \leq \varepsilon\lambda_j = C_1\varepsilon/C_6S_jN$. Since $S_j \geq \exp(-\alpha x_j/\varepsilon)$, we can write

$$\frac{h_j}{\varepsilon}\exp\left(\frac{-\alpha x_{j-1}}{\varepsilon}\right) \leq \frac{C_2}{C_6N}\exp\left(\frac{\alpha(x_j - x_{j-1})}{\varepsilon}\right).$$

Using (4.21) in the above expression, we get

$$\frac{h_j}{\varepsilon}\exp\left(\frac{-\alpha x_{j-1}}{\varepsilon}\right) \leq CN^{-1}. \tag{4.22}$$

Since $\exp(-\sigma/\varepsilon) = N^{-1}$. So from (4.20),

$$\begin{aligned}\exp\left(\frac{-x_{j-1}}{\varepsilon}\right) &= N^{-1}\exp\left(\frac{\sigma - x_{i-1}}{\varepsilon}\right)\\ &\leq N^{-1}\exp(C_7 + C_8) \leq CN^{-1}.\end{aligned} \tag{4.23}$$

Finally, from (4.22) and (4.23), we can conclude that

$$\left\{\min\left\{\frac{h_j}{\varepsilon}, 1\right\}\exp\left(\frac{-\alpha x_{j-1}}{\varepsilon}\right)\right\} \leq CN^{-1}, \tag{4.24}$$

and this completes the proof. □

We can now bound the ε-weighted error between the computed and the actual derivatives of the solution of (1.1).

Theorem 4.10. *There exist a constant C independent of ε and mesh points such that*

$$\max_{1\leq j\leq N} \varepsilon|D^-U_j^N - u'(x_j)| \leq CN^{-1}.$$

Proof. We know that $L^Ne_j = \tau_j$. From Lemma 3.1, we have

$$\varepsilon\|E\| \leq C|\tau_j| \leq C\max_{j=1,\ldots,N}\left\{\min\left\{\frac{h_j}{\varepsilon}, 1\right\}\exp\left(\frac{-\alpha x_{j-1}}{\varepsilon}\right)\right\} + CN^{-1}. \tag{4.25}$$

Using the inequality (4.24) in (4.25), we obtain the required estimate. □

4.4. Convergence of the global solution

The estimate given in Theorem 4.5 shows that the classical upwind scheme applied on the equidistributed grids is uniformly first-order accurate at all the mesh points. We can obtain the global approximation to the exact solution by interpolating the numerical solution at the mesh points using piecewise constant or piecewise linear functions. We now show that these global approximations are uniformly first-order accurate throughout the domain.

Theorem 4.11. *Let $\widetilde{u}(x)$ be the piecewise constant or piecewise linear interpolant of the solution U_j^N for the difference scheme (3.2) obtained on the grid (3.21). Then the global error satisfies the ε-uniform estimate*

$$\|u(x) - \widetilde{u}(x)\| \leq CN^{-1}. \tag{4.26}$$

Proof. Let $\widetilde{u}(x)$ denote the piecewise polynomial interpolant of degree k with either $k = 0$ or $k = 1$ where $x \in (x_{j-1}, x_j)$. Then

$$\widetilde{u}(x) = \begin{cases} U_j^N \chi_j(x), & k = 0, \\ U_{j-1}^N \phi_{j-1}(x) + U_j^N \phi_j(x), & k = 1, \end{cases} \tag{4.27}$$

where

$$\chi_j(x) = \begin{cases} 1, & \text{if } x \in (x_{j-1}, x_j), \\ 0, & \text{otherwise}, \end{cases}$$

and $\phi_{j-1}(x)$, $\phi_j(x)$ are Lagrange's interpolating polynomials of first degree given by

$$\phi_{j-1}(x) = \frac{x_j - x}{x_j - x_{j-1}}, \qquad \phi_j(x) = \frac{x - x_{j-1}}{x_j - x_{j-1}}.$$

For $k = 0$, we have

$$\begin{aligned} \widetilde{u}(x) - u(x) &= U_j^N \chi_j(x) - u(x_j) + u(x_j) - u(x) \\ &= U_j^N - u(x_j) + \int_x^{x_j} u'(s)\mathrm{d}s. \end{aligned}$$

For $k = 1$, we have

$$\begin{aligned} \widetilde{u}(x) - u(x) &= U_{j-1}^N \phi_{j-1}(x) + U_j^N \phi_j(x) - u(x) \\ &= [U_{j-1}^N - u(x_{j-1})]\phi_{j-1}(x) + [U_j^N - u(x_j)]\phi_j(x) - \phi_{j-1}(x) \int_{x_{j-1}}^{x} u'(s)\mathrm{d}s + \phi_j(x) \int_x^{x_j} u'(s)\mathrm{d}s. \end{aligned}$$

Using Theorem 4.5, we can conclude that

$$|\widetilde{u}(x) - u(x)| \leq \begin{cases} CN^{-1} + \displaystyle\int_x^{x_j} |u'(s)|\mathrm{d}s, & \text{if } k = 0, \\ CN^{-1} + C \displaystyle\int_{x_{j-1}}^{x_j} |u'(s)|\mathrm{d}s, & \text{if } k = 1. \end{cases}$$

Now we have to find the bound for the integral

$$I_j = \int_{x_{j-1}}^{x_j} |u'(s)|\mathrm{d}s.$$

Using (2.7) and the equidistribution principle (3.16), we may conclude that

$$\begin{aligned} I_j &\leq C\varepsilon^{-1} \int_{x_{j-1}}^{x_j} \exp(-\alpha s/m\varepsilon)\mathrm{d}s \\ &\leq \int_{x_{j-1}}^{x_j} \sqrt{1 + (u'(s))^2}\mathrm{d}s = \frac{1}{N} \int_0^1 M(u(s), s)\mathrm{d}s \\ &\leq \frac{C\ell}{N} \leq CN^{-1}. \end{aligned}$$

Hence, the required result follows. □

4.5. Error in the global normalized flux

The bound given in Theorem 4.10 gives the estimate for the pointwise error in the normalized flux defined by $\varepsilon u'(x)$. Here, in the following theorem, we are proving the uniform convergence estimate for the global normalized flux.

Theorem 4.12. *Let $u(x)$ be the solution of (1.1) and $\widetilde{u}(x)$ be the global solution defined as in (4.27). Then, the error of the normalized flux satisfies*

$$\varepsilon|u'(x_j) - \widetilde{u}'(x_j)| \leq CN^{-1}, \quad j = 0, \ldots, N. \tag{4.28}$$

Proof. For constant interpolant, we can get the required bound using Theorem 4.10. Now for the case of linear interpolant defined in (4.27), we have

$$\widetilde{u}'(x_j) = \frac{U_j^N - U_{j-1}^N}{h_j}.$$

Using the Taylor series expansion, we obtain that

$$\varepsilon|u'(x_j) - \widetilde{u}'(x_j)| \leq \frac{C\varepsilon}{h_j}\left[|u(x_{j-1}) - U_{j-1}^N| + |u(x_j) - U_j^N|\right] + C\varepsilon h_j|u''(\xi)|, \tag{4.29}$$

where $\xi \in (x_{j-1}, x_j)$. Now we distinguish the following two cases.

Case (i). $h_j = \mathcal{O}(\varepsilon)$ (*i.e.,* for the mesh points inside the layer region). Using the bound for the error given in Theorem 4.5, the inequality (4.29) can be bounded as

$$\varepsilon|u'(x_j) - \widetilde{u}'(x_j)| \leq CN^{-1} + C\varepsilon^2|u''(\xi)|.$$

Now using the bound of $u(x)$ given in Lemma 2.3, we can obtain the required estimate, *i.e.,*

$$\varepsilon|u'(x_j) - \widetilde{u}'(x_j)| \leq CN^{-1}.$$

Case (ii). On the other hand, when $h_j \leq CN^{-1}$ (*i.e.,* for the mesh points outside the layer region), using Theorem 4.5, we obtain

$$\varepsilon|u'(x_j) - \widetilde{u}'(x_j)| \leq CN^{-1} + C\varepsilon N^{-1}|u''(\xi)|.$$

Finally, using the assumption (1.2) *i.e.,* $\varepsilon \leq CN^{-1}$ and the bound given in Lemma 2.3, we can obtain the required result. □

5. Numerical results

In this section to validate the theoretical results, we apply the proposed numerical scheme to several test problems with constant and variable coefficients having left and right boundary layers. For comparison purposes, we use the upwind differences scheme on the piecewise-uniform Shishkin mesh.

Example 5.1. Consider the test problem

$$\begin{cases} -\varepsilon u''(x) - u'(x) + u(x) = 0, & x \in (0, 1), \\ u(0) = 0, \qquad u(1) = 1. \end{cases}$$

The exact solution is given by

$$u(x) = \frac{\exp(m_1 x) - \exp(m_2 x)}{\exp(m_1) - \exp(m_2)}, \quad \text{where } m_{1,2} = \frac{-1 \pm \sqrt{1 + 4\varepsilon}}{2\varepsilon}.$$

This BVP has a boundary layer in the left end at $x = 0$.

Example 5.2. Consider the variable coefficient problem

$$\begin{cases} -\varepsilon u''(x) - \big(1 + x(1 - x)\big)u'(x) = f(x), & x \in (0, 1), \\ u(0) = 0, \qquad u(1) = 0, \end{cases}$$

where $f(x)$ is chosen in such that its solution $u(x)$ is of the form

$$u(x) = \frac{1 - \exp(-x/\varepsilon)}{1 - \exp(-1/\varepsilon)} - \cos\left(\frac{\pi}{2}(1 - x)\right).$$

The above problem has a boundary layer at the left side of the domain near $x = 0$.

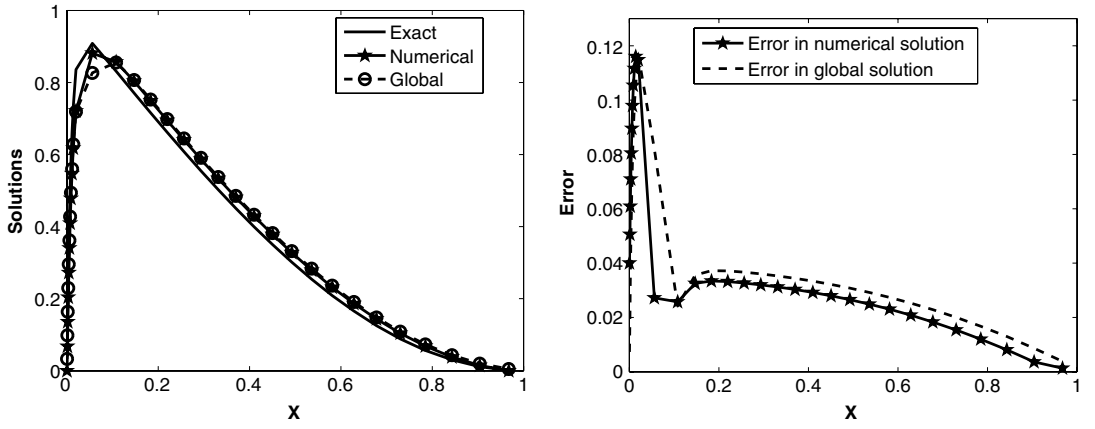

(a) Solution. (b) Error.

Fig. 1. Numerical solution and the global solution with the exact solution and the corresponding errors for Example 5.2 with $\varepsilon = 1e-2$ and $N = 32$.

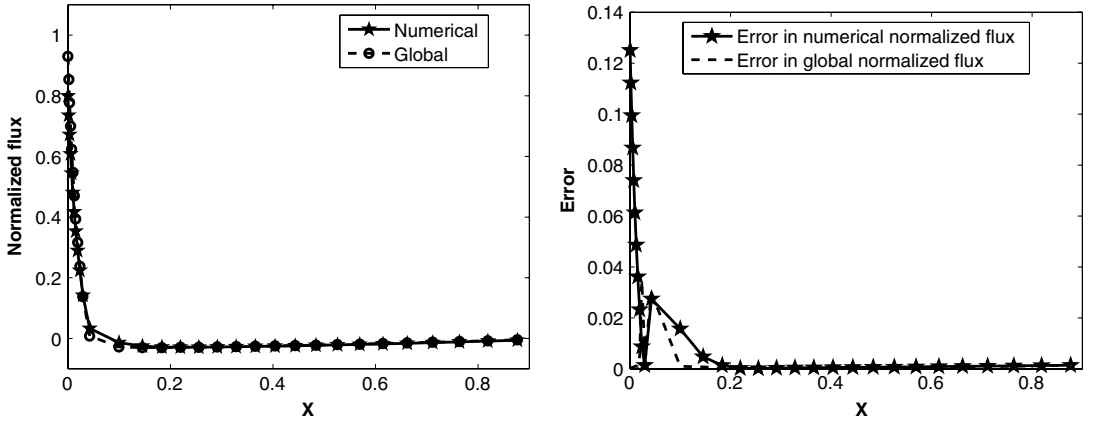

(a) Normalized flux. (b) Error in the normalized flux.

Fig. 2. Normalized flux and the error in the normalized flux for Example 5.2 with $\varepsilon = 1e-2$ and $N = 32$.

For boundary layer on the left, the piecewise-uniform Shishkin mesh $\overline{\Omega}_\varepsilon^N$ is constructed by partitioning the domain $[0, 1]$ into two subdomains $[0, \tau)$ and $[\tau, 1]$. τ is the point of transition from a fine mesh to the coarse mesh and is defined as $\tau = \min\{1/2, \tau_0 \varepsilon \ln N\}$, $\tau_0 = 1/\alpha$, where α defined earlier. The definition of τ guarantees the existence of some points inside the layer region. Without loss of generality, assume that N is even. Now we will place $N/2$ numbers of subintervals in each of the subdomains. The corresponding Shishkin mesh for the right boundary layer can be constructed in a similar fashion by dividing the domain into two subdomains $[0, 1-\tau]$ and $(1-\tau, 1]$ and placing $N/2$ number of intervals in each subdomain.

For any value of N and ε, we calculate the exact maximum pointwise errors E_ε^N and the corresponding rates of convergence by

$$E_\varepsilon^N = \max_{0\le j\le N} |u(x_j) - U_j^N| \quad \text{and} \quad r_\varepsilon^N = \log_2\left(\frac{E_\varepsilon^N}{E_\varepsilon^{2N}}\right),$$

where u is the exact solution and U_j^N is the numerical solution obtained by using N mesh intervals in the domain $\overline{\Omega}^N$.

Now we would like to see the errors associated with the global solution and with the weighted derivatives. To do that, we calculate the maximum errors at the midpoints $x_j^* = (x_j + x_{j+1})/2$, of the corresponding adaptive mesh. The errors associated with the global solution and the corresponding rates of convergence are obtained by

$$\widetilde{E}_\varepsilon^N = \max_{x_j^*\in\overline{\Omega}^N} \varepsilon|u(x_j^*) - \widetilde{u}(x_j^*)| \quad \text{and} \quad \widetilde{r}_\varepsilon^N = \log_2\left(\frac{\widetilde{E}_\varepsilon^N}{\widetilde{E}_\varepsilon^{2N}}\right),$$

Table 1
Maximum errors and the corresponding rate of convergence for Example 5.1.

ε	Number of intervals N						
		32	64	128	256	512	1024
1e−0	E_ε^N	1.8581e−3	9.3979e−4	4.7263e−4	2.3702e−4	1.1868e−4	5.9385e−5
	r_ε^N	0.9834	0.9916	0.9957	0.9978	0.9989	
	$\widetilde{E}_\varepsilon^N$	1.9822e−3	9.7129e−4	4.8056e−4	2.3900e−4	1.1918e−4	5.9509e−5
	$\widetilde{r}_\varepsilon^N$	1.0291	1.0152	1.0077	1.0039	1.0019	
1e−2	E_ε^N	8.8525e−2	4.9365e−2	2.9749e−2	1.3796e−2	7.7305e−3	3.8790e−3
	r_ε^N	0.8426	0.7306	1.1086	0.8355	0.9949	
	$\widetilde{E}_\varepsilon^N$	9.1050e−2	4.9969e−2	2.9920e−2	1.3839e−2	7.7417e−3	3.8818e−3
	$\widetilde{r}_\varepsilon^N$	0.8656	0.7399	1.1124	0.8379	0.9959	
1e−4	E_ε^N	1.1167e−1	6.3034e−2	3.6250e−2	2.0689e−2	1.1791e−2	6.2814e−3
	r_ε^N	0.8250	0.7981	0.8090	0.8111	0.9085	
	$\widetilde{E}_\varepsilon^N$	1.1439e−1	6.3899e−2	3.6486e−2	2.0754e−2	1.1809e−2	6.2860e−3
	$\widetilde{r}_\varepsilon^N$	0.8400	0.8084	0.8140	0.8134	0.9096	
1e−8	E_ε^N	1.1267e−1	6.6210e−2	3.8084e−2	2.0875e−2	1.1736e−2	6.5254e−3
	r_ε^N	0.7670	0.7978	0.8674	0.8308	0.8467	
	$\widetilde{E}_\varepsilon^N$	1.1542e−1	6.7138e−2	3.8327e−2	2.0939e−2	1.1753e−2	6.5302e−3
	$\widetilde{r}_\varepsilon^N$	0.7817	0.8087	0.8721	0.8331	0.8478	

Table 2
Maximum errors associated with the normalized flux and the corresponding rate of convergence for Example 5.1.

ε	Number of intervals N						
		32	64	128	256	512	1024
1e−0	D_ε^N	9.0413e−3	4.6545e−3	2.3611e−3	1.1891e−3	5.9669e−4	2.9888e−4
	p_ε^N	0.9579	0.9791	0.9896	0.9948	0.9974	
	$\widetilde{D}_\varepsilon^N$	8.8040e−3	4.5960e−3	2.3466e−3	1.1855e−3	5.9579e−4	2.9866e−4
	$\widetilde{p}_\varepsilon^N$	0.9378	0.9698	0.9851	0.9926	0.9963	
1e−2	D_ε^N	1.3050e−1	7.3835e−2	4.3398e−2	2.0703e−2	1.1352e−2	5.7057e−3
	p_ε^N	0.8217	0.7667	1.0678	0.8669	0.9924	
	$\widetilde{D}_\varepsilon^N$	1.2532e−1	7.2484e−2	4.3023e−2	2.0614e−2	1.1328e−2	5.6998e−3
	$\widetilde{p}_\varepsilon^N$	0.7899	0.7526	1.0615	0.8638	0.9909	
1e−4	D_ε^N	1.5698e−1	9.0000e−2	5.1245e−2	2.8758e−2	1.6067e−2	8.4818e−3
	p_ε^N	0.8026	0.8125	0.8335	0.8399	0.9216	
	$\widetilde{D}_\varepsilon^N$	1.5055e−1	8.8314e−2	5.0791e−2	2.8635e−2	1.6033e−2	8.4730e−3
	$\widetilde{p}_\varepsilon^N$	0.7696	0.7981	0.8268	0.8367	0.9201	
1e−8	D_ε^N	1.5808e−1	9.3570e−2	5.3303e−2	2.8969e−2	1.6007e−2	8.7534e−3
	p_ε^N	0.7565	0.8118	0.8797	0.8558	0.8708	
	$\widetilde{D}_\varepsilon^N$	1.5161e−1	9.1824e−2	5.2831e−2	2.8844e−2	1.5973e−2	8.7443e−3
	$\widetilde{p}_\varepsilon^N$	0.7234	0.7975	0.8731	0.8527	0.8692	

where $u(x)$ is the exact solution and $\widetilde{u}(x)$ is the global solution. Similarly, we can define the pointwise errors associated with normalized flux as:

$$D_\varepsilon^N = \max_{1\le j\le N} |u'(x_j) - D^- U_j^N| \quad \text{and} \quad p_\varepsilon^N = \log_2\left(\frac{D_\varepsilon^N}{D_\varepsilon^{2N}}\right),$$

and the global error for the normalized flux as:

$$\widetilde{D}_\varepsilon^N = \max_{x_j^*\in\overline{\Omega}^N} \varepsilon|u'(x_j^*) - \widetilde{u}'(x_j^*)| \quad \text{and} \quad \widetilde{p}_\varepsilon^N = \log_2\left(\frac{\widetilde{D}_\varepsilon^N}{\widetilde{D}_\varepsilon^{2N}}\right).$$

Fig. 1(a) and (b) represent the global solution along with the exact solution and the corresponding error obtained on the adaptive grid for Example 5.2 respectively. Similarly Fig. 2(a) and (b) represent the normalized flux and the corresponding error. In Tables 1 and 2, we present the maximum pointwise error and the corresponding order of convergence for the solution and it derivatives of Example 5.1 respectively. Similar results are shown in Tables 3 and 4 for Example 5.2 which clearly shows that the proposed method is ε-uniform convergent of order one.

Table 3
Maximum errors and the corresponding rate of convergence for Example 5.2.

ε		Number of intervals N					
		32	64	128	256	512	1024
1e−0	E_ε^N	1.8695e−3	9.3934e−4	4.7082e−4	2.3570e−4	1.1792e−4	5.8979e−5
	r_ε^N	0.9929	0.9964	0.9982	0.9991	0.9995	
	$\widetilde{E}_\varepsilon^N$	2.0127e−3	9.7526e−4	4.7981e−4	2.3795e−4	1.1848e−4	5.9120e−5
	$\widetilde{r}_\varepsilon^N$	1.0453	1.0233	1.0118	1.0060	1.0032	
1e−2	E_ε^N	1.0544e−1	5.5846e−2	3.3356e−2	1.5908e−2	8.4806e−3	4.0269e−3
	r_ε^N	0.9169	0.7434	1.0682	0.9075	1.0745	
	$\widetilde{E}_\varepsilon^N$	1.1674e−1	5.6885e−2	3.3642e−2	1.5981e−2	8.4993e−3	4.0315e−3
	$\widetilde{r}_\varepsilon^N$	1.0372	0.7577	1.0739	0.9109	1.0760	
1e−4	E_ε^N	1.0115e−1	7.8402e−2	3.5465e−2	2.4687e−2	1.3366e−2	7.2825e−3
	r_ε^N	0.3675	1.1445	0.5226	0.8851	0.8761	
	$\widetilde{E}_\varepsilon^N$	1.0446e−1	7.9705e−2	3.5759e−2	2.4782e−2	1.3391e−2	7.2892e−3
	$\widetilde{r}_\varepsilon^N$	0.3901	1.1563	0.5290	0.8879	0.8774	
1e−8	E_ε^N	1.0148e−1	7.8716e−2	3.5681e−2	2.4508e−2	1.3250e−2	7.1047e−3
	r_ε^N	0.3664	1.1415	0.5418	0.8872	0.8991	
	$\widetilde{E}_\varepsilon^N$	11.0481e−1	8.0018e−2	3.5977e−2	2.4604e−2	1.3276e−2	7.1113e−3
	$\widetilde{r}_\varepsilon^N$	0.3893	1.1532	0.5482	0.8900	0.9006	

Table 4
Maximum errors associated with the normalized flux and the corresponding rate of convergence for Example 5.2.

ε		Number of intervals N					
		32	64	128	256	512	1024
1e−0	D_ε^N	8.1040e−3	4.2931e−3	2.2058e−3	1.1176e−3	5.6242e−4	2.8212e−4
	p_ε^N	0.9166	0.9607	0.9809	0.9906	0.9953	
	$\widetilde{D}_\varepsilon^N$	8.0120e−3	4.2878e−3	2.2065e−3	1.1180e−3	5.6256e−4	2.8216e−4
	$\widetilde{p}_\varepsilon^N$	0.9019	0.9585	0.9809	0.9908	0.9955	
1e−2	D_ε^N	1.5561e−1	8.4682e−2	4.9688e−2	2.4250e−2	1.2815e−2	6.1740e−3
	p_ε^N	0.8778	0.7692	1.0349	0.9202	1.0535	
	$\widetilde{D}_\varepsilon^N$	1.4837e−1	8.2838e−2	4.9172e−2	2.4126e−2	1.2782e−2	6.1662e−3
	$\widetilde{p}_\varepsilon^N$	0.8409	0.7525	1.0273	0.9164	1.0517	
1e−4	D_ε^N	1.5008e−1	1.1044e−1	5.2416e−2	3.4431e−2	1.8471e−2	9.9343e−3
	p_ε^N	0.4425	1.0751	0.6063	0.8984	0.8948	
	$\widetilde{D}_\varepsilon^N$	1.4232e−1	1.0792e−1	5.1836e−2	3.4249e−2	1.8423e−2	9.9215e−3
	$\widetilde{p}_\varepsilon^N$	0.3992	1.0579	0.5979	0.8945	0.8929	
1e−8	D_ε^N	1.5045e−1	1.1075e−1	5.2675e−2	3.4229e−2	1.8343e−2	9.7373e−3
	p_ε^N	0.4419	1.0722	0.6219	0.9000	0.9136	
	$\widetilde{D}_\varepsilon^N$	1.4266e−1	1.0823e−1	5.2090e−2	3.4048e−2	1.8295e−2	9.7248e−3
	$\widetilde{p}_\varepsilon^N$	0.3985	1.0550	0.6134	0.8961	0.9117	

We have also compared the computational results using adaptive mesh to the numerical results using the Shishkin mesh which are shown in Table 5 and in Table 6 with $\varepsilon = 1e{-}3$ and $\varepsilon = 1e{-}6$ for Example 5.2. From these results, one can observe that adaptive mesh produces errors almost of the same order as produced by using the Shishkin mesh. The advantage of this approach is that without any prior knowledge of the location of the boundary layer, we are able to generate an appropriate nonuniform mesh suitable for the layer type problems.

6. Conclusion

In this article, we presented the analysis of an upwind scheme for obtaining the global solution and the normalized flux for singularly perturbed BVPs of the form (1.1). The solution obtained on a suitable nonuniform adaptive grids based on equidistribution principle. The global solution is obtained using the constant or piecewise liner interpolants. We carried out the error analysis for the ε-weighted error for the derivatives for both the numerical solution and the global solution. It is shown that the errors converge at the rate of first-order, independently of the singular perturbation parameter. Numerical results obtained for some examples show that proposed scheme is of first-order accurate. Hence, the key result established

Table 5
Comparison of numerical results with Shishkin mesh for Example 5.2.

N		$\varepsilon = 10^{-3}$		$\varepsilon = 10^{-6}$	
		Shishkin mesh	Adaptive mesh	Shishkin mesh	Adaptive mesh
64	E_ε^N	2.9727e−2	5.9218e−2	2.9662e−2	6.0498e−2
	r_ε^N	0.6307	0.4734	0.6315	0.7764
	$\widetilde{E}_\varepsilon^N$	3.2816e−2	6.0233e−2	3.2746e−2	6.1490e−2
	$\widetilde{r}_\varepsilon^N$	0.6873	0.4860	0.6878	0.7879
128	E_ε^N	1.9200e−2	4.2652e−2	1.9147e−2	3.5320e−2
	r_ε^N	0.7041	0.9632	0.7042	0.5356
	$\widetilde{E}_\varepsilon^N$	2.0379e−2	4.3006e−2	2.0329e−2	3.5616e−2
	$\widetilde{r}_\varepsilon^N$	0.7453	0.9695	0.7455	0.5421
256	E_ε^N	1.1785e−2	2.1877e−2	1.1752e−2	2.4365e−2
	r_ε^N	0.7594	0.9396	0.7595	0.8601
	$\widetilde{E}_\varepsilon^N$	1.2157e−2	2.1963e−2	1.2125e−2	2.4459e−2
	$\widetilde{r}_\varepsilon^N$	0.7799	0.9425	0.7800	0.8629
512	E_ε^N	6.9618e−3	1.1406e−2	6.9421e−3	1.3423e−2
	r_ε^N	0.7976	0.9339	0.7976	0.8808
	$\widetilde{E}_\varepsilon^N$	7.0807e−3	1.1428e−2	7.0613e−3	1.3449e−2
	$\widetilde{r}_\varepsilon^N$	0.8087	0.9354	0.8088	0.8823

Table 6
Comparison of flux results with Shishkin mesh for Example 5.2.

N		$\varepsilon = 10^{-3}$		$\varepsilon = 10^{-6}$	
		Shishkin mesh	Adaptive mesh	Shishkin mesh	Adaptive mesh
64	D_ε^N	6.8247e−2	8.8884e−2	6.8135e−2	9.0495e−2
	r_ε^N	0.4742	0.5556	0.4744	0.7924
	$\widetilde{D}_\varepsilon^N$	4.4718e−2	8.6834e−2	4.4621e−2	8.8382e−2
	$\widetilde{p}_\varepsilon^N$	0.1888	0.5376	0.1887	0.7743
128	D_ε^N	4.9129e−2	6.0476e−2	4.9041e−2	5.2252e−2
	r_ε^N	0.6147	0.9532	0.6147	0.6168
	$\widetilde{D}_\varepsilon^N$	3.9233e−2	5.9823e−2	3.9151e−2	5.1673e−2
	$\widetilde{p}_\varepsilon^N$	0.4670	0.9451	0.4669	0.6084
256	D_ε^N	3.2085e−2	3.1236e−2	3.2026e−2	3.4074e−2
	r_ε^N	0.7101	0.9433	0.7101	0.8781
	$\widetilde{D}_\varepsilon^N$	2.8383e−2	3.1071e−2	2.8327e−2	3.3894e−2
	$\widetilde{p}_\varepsilon^N$	0.6301	0.9394	0.6299	0.8742
512	D_ε^N	1.9613e−2	1.6244e−2	1.9577e−2	1.8539e−2
	r_ε^N	0.7734	0.9428	0.7733	0.8987
	$\widetilde{D}_\varepsilon^N$	1.8340e−2	1.6202e−2	1.8305e−2	1.8491e−2
	$\widetilde{p}_\varepsilon^N$	0.7294	0.9409	0.7293	0.8968

here is that the global solution and the normalized flux computed on the adaptive grids are uniformly convergent with respect to the perturbation parameter.

Acknowledgement

The first author wishes to thank Council of Scientific and Industrial Research [CSIR], Government of India, (Grant No-9/731(0071)/08-EMRI) for providing senior research fellowship for pursuing Ph.D. at Indian Institute of Technology Guwahati.

References

[1] M.G. Beckett, J.A. Mackenzie, Convergence analysis of finite differences approximations on equidistributed grids to a singularly perturbed boundary value problem, Appl. Numer. Math. 35 (166) (2000) 87–109.
[2] R.B. Kellogg, A. Tsan, Analysis of some difference approximations for a singular perturbation problem without turning point, Math. Comp. 32 (144) (1978) 1025–1039.

[3] J. Mohapatra, S. Natesan, Uniform convergence analysis of finite difference scheme for singularly perturbed delay differential equation on an adaptively generated grid, Numer. Math. Theory Methods Appl. 3 (1) (2010) 1–22.
[4] Y. Qiu, D.M. Sloan, T. Tang, Numerical solution of a singularly perturbed two point boundary value problem using equidistribution: analysis of convergence, J. Comput. Appl. Math. 116 (2000) 121–143.
[5] H.G. Roos, M. Stynes, L. Tobiska, Numerical Methods for Singularly Perturbed Differential Equations, Springer, Berlin, 1996.
[6] R.K. Bawa, C. Clavero, Higher order global solution and normalized flux for singularly perturbed reaction–diffusion problems, Appl. Math. Comput. 216 (7) (2010) 2058–2068.
[7] C. Clavero, R.K. Bawa, S. Natesan, A robust second-order numerical method for global solution and global normalized flux for singularly perturbed self-adjoint boundary value problems, Int. J. Comput. Math. 86 (10–11) (2009) 1731–1745.
[8] V. Ervin, W. Layton, On the approximation of the derivatives of singularly perturbed boundary value prblems, SIAM J. Sci. Comput. 8 (3) (1987) 265–277.
[9] N. Kopteva, M. Stynes, Approximation of derivatives in a convection–diffusion two-point boundary value problem, Appl. Numer. Math. 39 (2001) 47–60.
[10] S. Natesan, R.K. Bawa, C. Clavero, Uniformly convergent compact numerical scheme for the normalized flux of singularly perturbed reaction–diffusion problems, Int. J. Inf. Syst. Sci. 3 (2) (2007) 207–221.
[11] P.A. Farrell, A.F. Hegarty, J.J.H. Miller, E. O'Riordan, G.I. Shishkin, Robust Computational Techniques for Boundary Layers, Chapman & Hall/CRC Press, Boca Raton, FL, 2000.
[12] J. Mackenzie, Uniform convergence analysis of an upwind finite difference approximation of a convection–diffusion boundary value problem on an adaptive grid, IMA J. Numer. Anal. 19 (1999) 233–249.
[13] Y. Chen, Uniform convergence analysis of finite difference approximations for singularly perturbation problems on an adapted grid, Adv. Comput. Math. 24 (2006) 197–212.
[14] J.J.H. Miller, E. O'Riordan, G.I. Shishkin, Fitted Numerical Methods for Singular Perturbation Problems, World Scientific, Singapore, 1996.